

Influence of aggregate grading upon concrete tensile strength: a stereological analysis

A. Carpinteri, P. Cornetti & S. Puzzi

Politecnico di Torino, Department of Structural and Geotechnical Engineering, Corso Duca degli Abruzzi 24, 10129 Torino, Italy

ABSTRACT: The present paper provides a theoretical explanation of the *size effect* on concrete tensile strength based on a statistics of extremes approach to the aggregate size distribution, expressed as probability density function of the grains diameter (namely, the Füller truncated distribution). Since the weakest link in normal strength concrete is usually represented by the interface between the cementitious matrix and the aggregates, if we assume that the strength of the material depends on the largest flaw, we compute the probability density function of the strength as a function of the specimen size. In this way, we obtain –by a truncated distributions statistical approach– a size effect that substantially agrees with the multifractal scaling law (MFSL) for concrete tensile strength. Eventually, particular attention is paid to the computation of the power law exponent characterising the strength scaling at the smallest sizes.

Keywords: size-scale effect, multifractal scaling, stereology, truncated distributions, statistics of extremes

1 INTRODUCTION

With *size effect* we mean the dependence of one or more material parameters on the size of the structure made by that material. It is easy to realize the importance of this topic in engineering design. Recently, the scientific community dedicated significant efforts in order to have a precise description of this phenomenon and to highlight the physical mechanisms that lie behind it. Dealing specifically with concrete structures, it was seen that tensile strength decreases with the structural size, whereas fracture energy increases. In other words, the larger is the structure, the more brittle is its structural behaviour. The increase of brittleness with the structural size is mainly due to the localization of damage in the failure process of structures composed by quasi-brittle materials. Nowadays, the most used model to describe damage localization in materials with disordered microstructure (also called quasi-brittle or concrete-like materials) is the *cohesive crack model*, introduced by Hillerborg et al. (1976).

According to Hillerborg's model, the material is characterized by a stress-strain relationship (σ - ε), valid for the unbroken zones (Fig. 1a), and by a stress-crack opening displacement relationship (σ - w , the cohesive law), describing how the stress decreases from its maximum value σ_u to zero as the distance between the crack lips increases from zero to the critical displacement w_c (Fig. 1b). The area below the cohesive law represents the energy G_F spent to create the unit crack surface. The cohesive crack model is able to simulate tests where high stress gradients are present, e.g. tests on pre-notched specimens. On the other hand, relevant scale effects are encountered also in uniaxial tensile tests on dog-bone shaped specimens (Carpinteri & Ferro 1994, Van Mier & Van Vliet 1999) (see Fig. 2a), where smaller stress gradients are present. Figure 2b clearly shows that the cohesive law and its parameters G_F and σ_u are size-dependent. For this kind of tests, size effects should be ascribed to the material behaviour rather than to the stress-intensification. However, they cannot be predicted by the cohesive crack model.

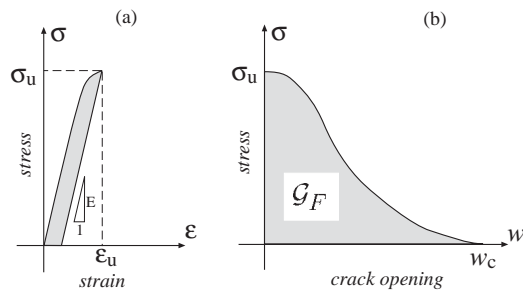


Figure 1. Hillerborg's cohesive crack model.

In order to overcome the original cohesive crack model drawbacks, a scale-independent (or fractal) cohesive crack model has been proposed recently (Carpinteri et al. 2002a). This model is based on the assumption of a fractal-like damage localization. The hypothesis of damage domains showing fractal patterns received previous experimental confirmations (Carpinteri et al. 1997a, 1999, 2001). The fractal nature of the damage process allows a consistent explanation of the size effect on the cohesive crack model parameters. In fact, if the damage zone is fractal, all the geometrical quantities (i.e. area of the resistant cross section, area of the crack surface and thickness of the damaged band) and all the physical quantities involved (i.e. tensile strength, fracture energy and critical displacement) depend on the measure resolution. Considering, for instance, the crack surface, it is seen that its area increases more and more as a larger number of details can be captured; as a consequence, the fracture energy decreases at higher resolution. In order to work with scale-invariant parameters one has to introduce fractal geometrical measures and fractal physical quantities. The fractal strength and fractal fracture energy were introduced by Carpinteri (1994a), while the fractal critical strain has been introduced more recently (Carpinteri et al. 2002a, 2002b). On the other hand, simple power laws describe the scale dependency of the fracture energy, tensile strength and critical displacement, the exponents being related to the fractal dimension of damage domains.

In order to get a better description of the size effect on concrete parameters over a broad range of scales, the notion of self-affinity was included in the previous model, the so-called multifractal scaling laws (MFSLs) for tensile strength, fracture energy and critical displacement (Carpinteri &

Chiaia 1997b, Carpinteri et al. 2003). Accordingly, the scaling laws are no longer simple power laws since they present a horizontal asymptote for the larger sizes, the fractal regime being valid only at the smaller sizes.

Aim of the present paper is the evaluation of the tensile strength of a concrete structure based on the hypothesis that the largest flaw is the cause of the specimen failure. Furthermore, since the interface between the cementitious matrix and the aggregates is the weakest link in concrete, we assume that a penny shaped crack with diameter equal to the maximum diameter of the grains inside the specimen can represent the largest flaw. It is evident that, for very large sizes, the diameter of the largest flaw coincides with the maximum diameter ϕ_{max} of the aggregate size distribution, i.e., the tensile strength shows an asymptote at the larger scales. On the other hand, the smaller is the specimen, the smaller is the maximum grain and the higher is the strength.

From a statistical point of view, the problem is represented by the computation of the probability density function (pdf) of the diameter of the largest grain inside a specimen containing a given number of grains, i.e. a classical extremes statistics problem. Regarding this mathematical topic, we refer to the milestone book of Gumbel (1958). In order to perform the statistical analysis, differently from Carpinteri et al. (1997c) where arbitrary truncated flaw distributions were used, we use a specific truncated distribution (namely the Fuller distribution) that describes the flaw population realistically. We use some formulae from Stereology, which encompasses the geometrical probability aspects of the problem; for what concerns stereology applied to concrete, we refer to the work by Stroeven (2000).

Eventually, the excellent agreement between the size effect upon the tensile strength predicted by the present analysis and the one predicted by the multifractal scaling law (MFSL) proposed by Carpinteri (1994b) and Carpinteri & Chiaia (1997b) will be shown and discussed.

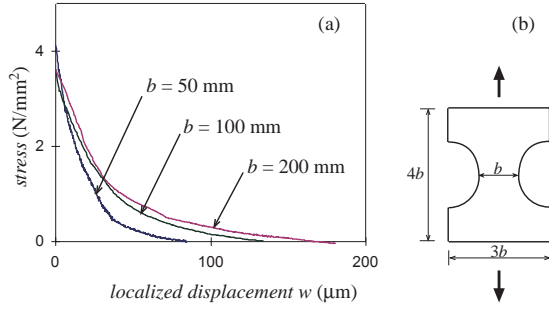


Figure 2. Uniaxial tensile tests over dog-bone shaped specimens: cohesive laws for different specimen sizes (a) and specimen shape (b).

2 STEREOLOGICAL ANALYSIS OF THE GRAIN SIZE DISTRIBUTION FUNCTION

In this section we will compute the average value of the largest flaw inside a given concrete volume.

The basis for the dimensional characterization of the concrete aggregate is the sieve analysis. The sieve curve describes the weight fraction $W(d)$ of the aggregate passing through a sieve with d -wide mesh. Due to its good packing properties, the most common sieve curve used to prepare concrete is the so-called Füller curve:

$$W(d) = \sqrt{\frac{d}{\phi_{\max}}} \quad (1)$$

Henceforth we will refer always to the Füller aggregate size distribution. Furthermore, we will assume the aggregates to be spheres with diameter d comprised between ϕ_{\min} and ϕ_{\max} . Common values for ϕ_{\min} and ϕ_{\max} are respectively 0.2 mm and 20 mm, even if, in large buildings, the largest diameter can be proportional to the size of the structure (till 120 mm).

It can be easily shown (Stroeven 2000) that the Füller sieve curve (Equation 1) can be expressed in terms of grain size distribution function (probability density function of the grain diameter, hereafter indicated as pdf) as follows:

$$f_d(d) = \frac{2.5}{1-\alpha^{-2.5}} \frac{\phi_{\min}^{2.5}}{d^{3.5}} \quad (2)$$

where $\alpha = \phi_{\max}/\phi_{\min}$ and $f_d(d)$ is a probability density function (herein indicated with small f), i.e. $f_d(d) dd$ is the relative number of grains with diameter belonging to the interval $[d, d + dd]$. Obviously, the integral of the pdf $f_d(d)$ over the whole diameter interval $[\phi_{\min}, \phi_{\max}]$ is equal to 1.

Equation 2 shows clearly that the number of small particles is higher than that of the larger ones, since the former must fill the gaps between the latter ones. Note that the first denominator in the previous expression is very close to the unity; nevertheless, differently from other approaches (Stroeven 2000), we cannot neglect it in the following computation since that term will be raised to very high exponents.

Our analysis needs the first three moments of the probability density function (Equation 2). The first moment represents the average diameter in the concrete volume, while the second and third are proportional to the average grain area and volume:

$$\bar{d} = \int_{\phi_{\min}}^{\phi_{\max}} f_d(d) d dd = \frac{5(1-\alpha^{-1.5})}{3(1-\alpha^{-2.5})} \phi_{\min} \quad (3)$$

$$\overline{d^2} = \int_{\phi_{\min}}^{\phi_{\max}} f_d(d) d^2 dd = \frac{5(1-\alpha^{-0.5})}{(1-\alpha^{-2.5})} \phi_{\min}^2 \quad (4)$$

$$\overline{d^3} = \int_{\phi_{\min}}^{\phi_{\max}} f_d(d) d^3 dd = \frac{5(1-\alpha^{-0.5})}{(1-\alpha^{-2.5})} \phi_{\min}^{2.5} \phi_{\max}^{0.5} \quad (5)$$

In order to find the relationship between concrete volume and number of grains inside it, we need one more parameter, i.e., the volume percentage f_a of the aggregates. This percentage must be high even if not too high, since the aim is a good particle packing but also a sufficient fluidity of the mixture when the concrete is cast. In normal strength concrete the aggregates occupy about three fourths of the total volume; hence $f_a \cong 0.75$. The total number of particles inside the cube of side b and volume $V=b^3$ is, therefore, on average:

$$N = \frac{f_a V}{\frac{\pi}{6} d^3} \quad (6)$$

This means that, when the above data are considered, the particles inside 1 m^3 of concrete are about 4 billions! Equation 6 gives a connection between structure volume and number of aggregate particles and will be widely used in the following, being crucial in the asymptotic analysis and in the calculus of the ultimate strength scaling law exponent.

To compute the average value of the largest flaw inside the specimen, we need to pass from the probability density functions f to the cumulative distribution functions, which are indicated with capital F . The cumulative distribution function of the aggregate particle diameter is defined as the

integral of the probability density function (Equation 2):

$$F_d(d) = \int_{\phi_{\min}}^d f_d(x) dx = \frac{1 - \left(\frac{\phi_{\min}}{d}\right)^{2.5}}{1 - \alpha^{-2.5}} \quad (7)$$

Our aim is now to find the expression of the probability density function of the maximum diameter of the N aggregate particles contained within the structure, defined as: $d_{\max} = \max\{d_1, d_2, \dots, d_N\}$. Each particle diameter can be considered as a statistical variable. A fundamental hypothesis is that all these variables are i.i.d. (independent and identically distributed); this is not unnatural, because they come all from the same distribution (Equation 2), related to the Füller sieve curve. Working on the cumulative distribution function, this assumption leads to the following equality chain, where $P[\text{event}]$ represents the probability of that event to occur:

$$\begin{aligned} F_{d_{\max}}(d) &= P[d_{\max} \leq d] = \prod_{i=1}^N P[d_i \leq d] = \\ &= \prod_{i=1}^N F_{d_i}(d) = [F_d(d)]^N \end{aligned} \quad (8)$$

where the second equality is justified by the independence and the last by the identical distribution assumption. By derivation it is now possible calculating the probability density function of d_{\max} .

$$f_{d_{\max}}(d) = \frac{d}{d(d)} [F_{d_{\max}}(d)] = N [F_d(d)]^{N-1} f_d(d) \quad (9)$$

Based on the hypothesis that the strength depends on the largest flaw, i.e. under Weibull's "weakest link" assumption, and assuming that defect interactions are negligible, if we represent the effect of a spherical aggregate particle as that of a penny shaped crack with the same diameter, we can write the ultimate tensile strength as:

$$\sigma_u(d_{\max}) = \frac{\pi}{2} \frac{K_{IC}}{\sqrt{\pi d_{\max}}} \quad (10)$$

The tensile strength σ_u is therefore a statistical variable as well as d_{\max} . The pdf f_{σ_u} of σ_u depends on the pdf of d_{\max} according to the relationship:

$$f_{\sigma_u}(\sigma_u) = f_{d_{\max}}(d) \left| \frac{d d_{\max}}{d \sigma_u} \right| \quad (11)$$

In order to obtain the average value of the ultimate tensile strength σ_u , the following integral needs to be evaluated:

$$\overline{\sigma_u} = \int_{\sigma_{u_{\min}}}^{\sigma_{u_{\max}}} \sigma_u f_{\sigma_u}(\sigma_u) d\sigma_u \quad (12)$$

Through the variable change given by Equation 10 and using Equation 11, we get:

$$\overline{\sigma_u} = \int_{\phi_{\min}}^{\phi_{\max}} \frac{K_{IC} \sqrt{\pi}}{2} \frac{f_{d_{\max}}(d)}{\sqrt{d}} dd \quad (13)$$

f_t being the minimum tensile strength value, which is attained for $d_{\max} = \phi_{\max}$:

$$f_t = \frac{\pi}{2} \frac{K_{IC}}{\sqrt{\pi \phi_{\max}}} \quad (14)$$

Equation 13 can be set in dimensionless form:

$$\frac{\overline{\sigma_u}}{f_t} = \int_{\phi_{\min}}^{\phi_{\max}} \frac{f_{d_{\max}}(d)}{\sqrt{d/\phi_{\max}}} dd \quad (15)$$

Integrating by parts, we obtain:

$$\begin{aligned} \frac{\overline{\sigma_u}}{f_t} &= \\ & \left[\sqrt{\frac{\phi_{\max}}{d}} F_{d_{\max}}(d) \right]_{\phi_{\min}}^{\phi_{\max}} + \frac{1}{2} \int_{\phi_{\min}}^{\phi_{\max}} \sqrt{\frac{\phi_{\max}}{d^3}} F_{d_{\max}}(d) dd \end{aligned} \quad (16)$$

Equations 7 and 8 give:

$$\frac{\overline{\sigma_u}}{f_t} = 1 + \frac{1}{2} \int_{\phi_{\min}}^{\phi_{\max}} \sqrt{\frac{\phi_{\max}}{d^3}} \frac{\left[1 - \left(\frac{\phi_{\min}}{d}\right)^{2.5}\right]^N}{(1 - \alpha^{-2.5})^N} dd \quad (17)$$

Equation 17 can be simplified by setting $t = d/\phi_{\min}$:

$$\frac{\overline{\sigma_u}}{f_t} = 1 + \frac{\sqrt{\alpha}}{2(1 - \alpha^{-2.5})^N} \int_1^{\alpha} t^{-1.5} (1 - t^{-2.5})^N dt \quad (18)$$

The integral in Equation 18 cannot be solved in a closed form. In addition, if N is not small enough as in the case of concrete aggregates, its numerical evaluation becomes very difficult. In fact, if a binomial expansion of the argument is adopted, the numerical binomial coefficients become very large, leading to overflow errors and to cancellation problems due to the opposite signs of subsequent terms. For instance, if N is equal to one thousand, the binomial coefficients reach values of the order of 10^{299} , but N can be even greater! To overcome this problem we adopt another variable change. Setting $x = t^{-2.5}$, we obtain:

$$\frac{\overline{\sigma_u}}{f_t} = 1 + \frac{\sqrt{\alpha}}{5(1 - \beta)^N} \int_{\beta}^1 (1 - x)^N x^{-4/5} dx \quad (19)$$

where the lowest integration bound is defined as $\beta = \alpha^{-2.5}$. The following reduction formula for

integrals of binomial differentials can be applied to the integral in Equation 19:

$$\int (ax^n + b)^p x^m dx = \frac{1}{m+np+1} \left[x^{m+1} (ax^n + b)^p + npb \int x^m (ax^n + b)^{p-1} dx \right] \quad (20)$$

where a , b , p , m and n can be any number for which the denominator does not vanish. Note that Equation 20 is not the classical integration by parts formula, useless in the present case. Applying now Equation 20 N times to the integral in Equation 19, we obtain the sum of N positive terms, thus avoiding numerical cancellation problems, while the coefficient of the integral becomes zero. Collecting all terms and carefully observing their properties, a recursive formula for the integral can be derived:

$$\int_{\beta}^1 (1-x)^N x^{-4/5} dx = \frac{1}{N + \frac{1}{5}} \left(b_N - \frac{a_N}{\sqrt{\alpha}} \right) \quad (21)$$

where the coefficients b_N and a_N are defined by recursion:

$$a_0 = b_0 = 1 \quad (22a)$$

$$a_i = (1-\beta)^i + \frac{i}{i-\frac{4}{5}} a_{i-1} \quad (22b)$$

$$b_i = \frac{i}{i-\frac{4}{5}} b_{i-1} \quad (22c)$$

We are now able to express Equation 19 as:

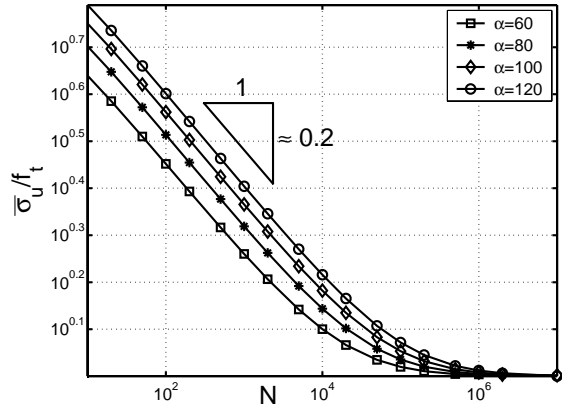


Figure 3. Ultimate strength as a function of number particles.

$$\frac{\overline{\sigma_u}}{f_t} = 1 + \frac{\sqrt{\alpha}}{(1-\beta)^N (5N+1)} \left(b_N - \frac{a_N}{\sqrt{\alpha}} \right) = f(\alpha, N) \quad (23)$$

The nondimensional mean value of the tensile strength can be calculated by Equation 23 as a function of the particles number N and of the parameter α . A first important remark is that only the ratio α between maximum and minimum aggregate size plays a role, whilst the value of the maximum diameter does not affect the function's shape. Results are summarized in Figure 3, where the log-log plot evidences that all the curves exhibit a similar behaviour, with two distinct ranges. In the lowest one the curves decrease with a constant slope, approximately equal to 0.2, thus following a power law, whilst for larger values of N they present an asymptotic trend towards the unity. Physically speaking, this means that increasing the number of particles considered, or, as stated by Equation 6, the corresponding structure volume, the probability of finding among them one with the maximum size approaches the unity, i.e. certainty. From a mechanical point of view, this yields an average tensile strength approaching f_t for sufficiently high N values.

3 SIZE EFFECT ON TENSILE STRENGTH

From the results obtained in the previous section, the following power law of tensile strength versus number of aggregate particles holds at small scales, i.e. for small numbers N :

$$\sigma_u \propto N^{-0.2} \quad (24)$$

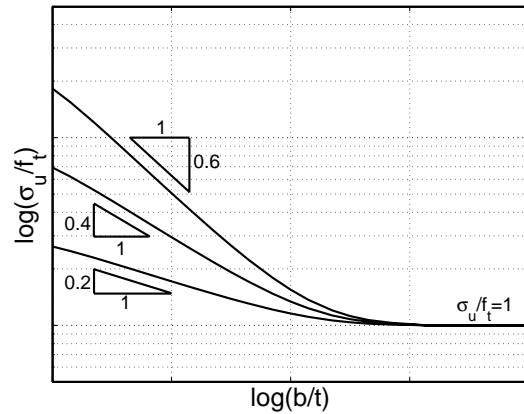


Figure 4. Size effect on tensile strength for one- two and three-dimensional structural scaling.

To highlight the scale effect on this parameter, the need emerges for expressing N as a function of a characteristic structural size b related to the

geometry of the specimen. We already know that the number of aggregate particles is related to the specimen volume V as expressed by Equation 6. We now introduce a characteristic structural length b , distinguishing three different cases:

1. One-dimensional scaling: $V \approx b^1$,
2. Two-dimensional scaling: $V \approx b^2$,
3. Three-dimensional scaling: $V \approx b^3$.

The consequent result is a set of different exponent values at small scales, whilst the behaviour at large scales is independent of the considered scaling type. The small-scale scaling are respectively the following:

1. One-dimensional scaling: $\sigma_u \approx b^{-0.2}$
2. Two-dimensional scaling: $\sigma_u \approx b^{-0.4}$
3. Three-dimensional scaling: $\sigma_u \approx b^{-0.6}$.

These three types of asymptotic behaviour are summarized in Figure 4. As it can be easily argued, the higher is the order of scaling, the stronger is the size-scale effect.

4 COMPARISON WITH EXPERIMENTAL DATA

In the last few years, a broad experimental research programme was carried out at the Politecnico di Torino by Carpinteri & Ferro (1994) to assess the scale effect on tensile tests of dog-bone shaped concrete specimens in a scale range of 1:16. They observed a relevant size-dependence of concrete tensile strength.

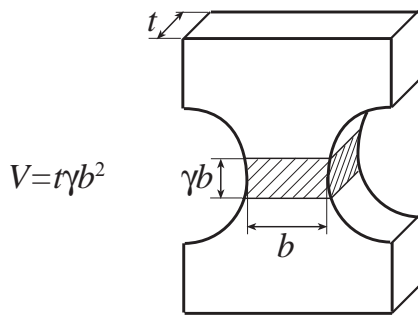


Figure 5. Dog-bone shaped specimen uniaxial tensile tests: volume where to seek the largest flaw

The scaling adopted was two-dimensional. The thickness t was kept constant and equal to 10 cm, whereas the ligament width varied from 2.5 to 40 cm; the specimen length was scaled proportionally (Figs 2a, 5). The aggregate grading was

characterised by an α value equal to 80. In order to apply Equation 23, we need to specify the volume V where the largest flaw should be sought. Of course, this is not the whole specimen volume, since only the flaws close to the middle cross section can cause failure. In fact, for hour-glass specimen, failure is caused by the unstable propagation of a main crack that takes place in a narrow band at the centre of the specimen, where the stress is uniform and higher than in the remaining part. The dominant crack starts from the largest flaw. Therefore, as shown in Figure 5, the volume can be expressed as:

$$V = b(\gamma b)t \quad (25)$$

γ being a coefficient related to the thickness of the zone where fracture can grow. Substituting Equation 25 into Equation 6 yields the expression for the nondimensional structural size b/t :

$$\frac{b}{t} = \sqrt{\frac{\pi N}{6 f_a \gamma} \left(\frac{d^3}{t^3} \right)} \quad (26)$$

Equation 26 together with Equation 23 describes the σ_u/f_t vs. b/t curve as a function of the parameter N . The resulting strength-scale relation is reported in Figure 6 together with experimental data. A best fit is performed varying the two parameters γ and f_t and the optimal values are approximately $\gamma = 0.06$ and $f_t = 3.98$ MPa. As is evident from the reported diagram, a satisfactory agreement has been found between the proposed scaling law and the experimental trends. According to the two-dimensional scaling, the slope in the bilogarithmic plot for small-scale strength size effect is 0.4.

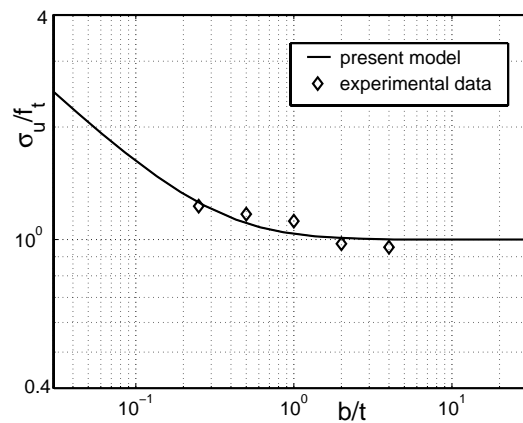


Figure 6. Dog-bone shaped specimen uniaxial tensile tests: comparison between the present model and experimental data (Carpinteri & Ferro 1994).

5 CONCLUSIONS

The experimental data cited in the previous section (Carpinteri and Ferro, 1994) and the observed size effects were explained by Carpinteri (1994a) assuming that the resistant ligament is a lacunar fractal (self-similar) set. This hypothesis yielded a power scaling law for tensile strength. The successive introduction of the self-affinity notion allowed a better description of the size effect on concrete parameters and led to the so-called multifractal scaling law (MFSL) for tensile strength (Carpinteri 1994b, Carpinteri & Chiaia 1997b). In this case, the scaling law is no longer a simple power law, but presents a horizontal asymptote for large sizes, while the fractal regime holds only at small scales:

$$\frac{\sigma_u}{f_t} = \left[1 + \frac{l_{ch}}{b} \right]^{+1/2} \quad (27)$$

where b is the characteristic dimension of the structure, l_{ch} is the internal length of the material and f_t is the large size asymptotic strength. It is interesting to point out that the stereological analysis presented in this paper, where we have made no use of fractal geometry concepts, yielded a scaling law (expressed by the couple of Equations 23-26) very similar to the MFSL (Equation 27). Both the scaling laws present a flat asymptote for large sizes (f_t) and a negative slope for small sizes equal to 0.5 for the MFSL and to 0.4–0.6 for the stereological analysis. In other words, we can affirm that, according to the stereological analysis, the scaling described by the MFSL reproduces satisfactorily the size effects of structures whose scaling is two- or three-dimensional.

Another remarkable aspect is that the present Weibull statistical approach can provide a much more complex scaling than a simple power law, thus resulting in the presence of an intrinsic characteristic length of the material. This is more than reasonable, due to the aggregate content of the material, and it overcomes the lack of a characteristic material length in the previous statistical theories on the ultimate strength (Freudentahl 1968, Evans 1978, Kittl & Diaz 1990).

In conclusion, it is useful to observe that the transition length (i.e. the structural dimension at which the size effect disappears) is given by l_{ch} in the MFSL (Equation 27), whereas it is a function of the maximum aggregate diameter in the present model – see Equation 26.

6 ACKNOWLEDGEMENTS

Support by the EC-TMR Contract No ERBFMRXCT 960062 is gratefully acknowledged by the authors. Thanks are also due to the Italian Ministry of University and Scientific Research.

7 REFERENCES

- Carpinteri, A. & Ferro, G. (1994). Size effects on tensile fracture properties: a unified explanation based on disorder and fractality of concrete microstructure. *Materials and Structures*, 28: 563-571.
- Carpinteri A. (1994a). Fractal nature of material microstructure and size effects on apparent mechanical properties. *Mechanics of Materials*, 18: 89-101.
- Carpinteri A. (1994b). Scaling laws and renormalization groups for strength and toughness of disordered materials. *International Journal of Solids and Structures*, 31: 291-302.
- Carpinteri, A., Chiaia, B. & Nematì, K.M. (1997a). Complex fracture energy dissipation in concrete under different loading conditions. *Mechanics of Materials*, 26: 93-108.
- Carpinteri, A. & Chiaia, B. (1997b). Multifractal scaling laws in the breaking behaviour of disordered materials. *Chaos, Solitons and Fractals*, 8: 135-150.
- Carpinteri, A., Ferro, G. & Invernizzi, S. (1997c). The nominal tensile strength of disordered materials: a statistical fracture mechanics approach. *Engineering Fracture Mechanics*, 58: 421-435.
- Carpinteri, A., Chiaia, B. & Invernizzi, S. (1999). Three-dimensional fractal analysis of concrete fracture at the meso-level. *Theoretical and Applied Fracture Mechanics*, 31: 163-172, 1999.
- Carpinteri A. & Invernizzi S. (2001). Influence of damage on the fractal properties of concrete subjected to pure tension. *Materials & Structures (R.I.L.E.M.)*, 34: 605-611.
- Carpinteri, A., Chiaia, B. & Cornetti, P. (2002a). A scale-invariant cohesive crack model for quasi-brittle materials. *Engineering Fracture Mechanics*, 69: 207-217.
- Carpinteri, A. & Cornetti, P. (2002b). A fractional calculus approach to the description of stress and strain localization in fractal media. *Chaos, Solitons and Fractals*, 13: 85-94.
- Carpinteri, A. & Cornetti, P. (2002c). Size effects on concrete tensile fracture properties: an

- interpretation of the fractal approach based on the aggregate grading. *Journal of the Mechanical Behaviour of Materials*, 13: 233-246.
- Carpinteri, A., Chiaia, B. & Cornetti, P. (2003). On the mechanics of quasi-brittle materials with a fractal microstructure, *Engineering Fracture Mechanics*, 70: 2321-2349.
- Evans, A.G. (1978). *A general approach for the statistical analysis of multiaxial fracture*, *Journal of the American Ceramic Society*, 61: 302-308.
- Freudentahl, A.M. (1968). Statistical approach to brittle fracture. In Liebowitz, H. (ed.), *Fracture*, Vol. 2: 591-619, Academic Press.
- Gumbel, E.J. (1958). *Statistics of extremes*, Columbia University Press, New York.
- Hillerborg, A., Modéer, M. & Petersson P.E. (1976). Analysis of crack formation and crack growth in concrete by means of fracture mechanics and finite elements. *Cement and Concrete Research*, 6: 773-782.
- Kittl, A. & Diaz, G. (1990). *Size effect on fracture strength in the probabilistic strength of materials*, *Reliability Engineering and System Safety*, 28: 9-21.
- van Mier, J.G.M. & van Vliet, M.R.A. (1999). Effect of strain gradients on the size effect of concrete in uniaxial tension. *International Journal of Fracture*, 94: 195-219.
- Stroeven, P. (2000). A stereological approach to roughness of fracture surfaces and tortuosity of transport paths in concrete. *Cement and Concrete Composites*, 22: 331-341.